Stem Cell Research & Therapy

RESEARCH

Open Access

NQO1 promotes osteogenesis and suppresses angiogenesis in DPSCs via MAPK pathway modulation

Wanqing Wang[1], Haoqing Yang[1], Zhipeng Fan[1,3,4*] and Ruitang Shi[2*]

Abstract

Background Influence on stem cells' angiogenesis and osteogenesis of NAD(P)H Quinone Dehydrogenase 1(NQO1) has been established, but its impact on dental pulp stem cells (DPSCs) is unexplored. An important strategy for the treatment of arteriosclerosis is to inhibit calcium deposition and to promote vascular repair and angiogenesis. This study investigated the function and mechanism of NQO1 on angiogenesis and osteogenesis of DPSCs, so as to provide a new ideal for the treatment of arteriosclerosis.

Methods Co-culture of human DPSCs and human umbilical vein endothelial cells (HUVECs) was used to detect the angiogenesis ability. Alkaline phosphatase (ALP) activity, alizarin red staining (ARS), and transplantation of HA/tricalcium phosphate with DPSCs were used to detect osteogenesis.

Results NQO1 suppressed in vitro tubule formation, migration, chemotaxis, and in vivo angiogenesis, as evidenced by reduced CD31 expression. It also enhanced ALP activity, ARS, DSPP expression and osteogenesis and boosted mitochondrial function in DPSCs. CoQ10, an electron transport chain activator, counteracted the effects of NQO1 knockdown on these processes. Additionally, NQO1 downregulated MAPK signaling, which was reversed by CoQ10 supplementation in DPSCs-NQO1sh.

Conclusions NQO1 inhibited angiogenesis and promoted the osteogenesis of DPSCs by suppressing MAPK signaling pathways and enhancing mitochondrial respiration.

Keywords NQO1, Angiogenesis, Osteogenesis, Mitochondrial respiration, DPSC

Introduction

Cardiovascular disease remains one of a leading cause of mortality in humans worldwide. Despite the significant progress made over the past decade, its pathogenesis and treatment require further exploration [1]. The common pathological basis of cardiovascular diseases is arteriosclerosis [2]. Arteriosclerosis can cause a decrease in blood supply, leading to decreased organ function in the area innervated by the artery, and even death. Arteriosclerosis starts from the intima and is accompanied by fibrous tissue hyperplasia and calcinosis, resulting in the thickening and hardening of the arterial wall and narrowing of the vascular cavity [3]. The inhibition of calcium deposition and promotion of vascular repair and

*Correspondence:
Zhipeng Fan
zpfan@ccmu.edu.cn
Ruitang Shi
shiruitang@126.com
[1] Beijing Key Laboratory of Tooth Regeneration and Function Reconstruction, Beijing Stomatological Hospital, School of Stomatology, Capital Medical University, Beijing 100050, China
[2] Department of Endodontics, Beijing Stomatological Hospital, School of Stomatology, Capital Medical University, Beijing 100050, China
[3] Beijing Laboratory of Oral Health, Capital Medical University, Beijing 100069, China
[4] Research Unit of Tooth Development and Regeneration, Chinese Academy of Medical Sciences, Beijing, China

formation are important strategies for the treatment of arteriosclerosis. However, the current treatment methods, including diet control, drug therapy, interventional therapy and bypass surgery, have limitations. Therefore, the treatment of arteriosclerosis is complex, time-consuming, and expensive. We urgently need to develop new treatments modalities.

Recently, some literatures have been reported that mesenchymal stem cells (MSCs) could be used to treat cardiovascular diseases [4, 5]. The therapeutic effects of MSCs on cardiovascular diseases are mainly related to the regeneration of blood vessels and cardiomyocytes. As a type of MSCs, dental pulp stem cells (DPSCs) are proven to be effective in the treatment of multiple diseases because of their strong self-renewal and multi-differentiation abilities, easy availability, and low immunogenicity. DPSCs can also be used to treat cardiovascular diseases because they can secrete pro-angiogenic and anti-apoptotic factors, promote angiogenesis, and also reduce the size of myocardial infarction [6, 7]. However, its stability and mechanism of action require further exploration.

The change of NQO1 gene expression may be related to the pathogenesis of coronary artery disease and is one of the risk genes for this kind of disease [8, 9]. NQO1 is a homologous dimeric flavinase that catalyzes the reduction of quinone to hydroquinone through a single-step, two-electron reduction reaction, thereby promoting quinone excretion and preventing oxidative damage to DNA caused by environmental stress [10],which may have a positive effect on cardiovascular disease as oxidative stress is a factor in the development of cardiovascular disease. As part of the antioxidant system, NQO1 can reduce oxidative stress, help protect vascular endothelial cells damaged by oxidative stress in the context of diabetes and hyperglycemia, and slow the development of vascular dysfunction and complications [11]. Through its antioxidant properties, NQO1 protects cells related to cardiovascular diseases, such as vascular smooth muscle cells [12], macrophages [13], fibroblasts [14], etc., from oxidative stress, which is one of the important mechanisms to maintain vascular health and prevent arteriosclerosis. NQO1 is critical in the osteogenesis of bone marrow mesenchymal stem cells (BMSCs) [15, 16] and the angiogenesis of human bone marrow endothelial cells [17]. However, it is unclear whether NQO1 affects osteogenesis and angiogenesis of DPSCs.

Reactive oxygen species (ROS) produced by mitochondria can cause oxidative stress and cell damage. NQO1 protects cells from oxidative stress by reducing oxidized substrates to their corresponding quinones [18]. Therefore, NQO1 exerts a regulatory effect on mitochondrial function. Mitochondria have been proven to be involved in osteogenesis by promoting osteoprogenitor differentiation [19]. Mitochondrial transfer from macrophages to MSCs promotes the osteogenic differentiation of MSCs [20]. The mitochondria also influence angiogenesis. Decreasing the expression of mitochondrial outer membrane proteins can inhibit angiogenesis by decreasing VEGFR2 expression [21]. However, whether NQO1 affects DPSC osteogenesis and angiogenesis by regulating mitochondrial function needs to be confirmed experimentally.

MAPK signaling pathway is particularly important in eukaryotic signal transmission networks. Several different MAPK signaling pathways have been identified, including Erk1/2, p38, JNK, and BMK1. These signaling pathways play different roles in regard to cell growth, differentiation, stress responses, and inflammatory response [22]. The MAPK signaling pathway is closely related to osteogenesis and angiogenesis [23]. Changes in mitochondrial function can affect cell function by altering the MAPK signaling pathway [24]. However, whether NQO1 affects the MAPK signaling pathway by regulating mitochondrial function requires further investigation. In view of this, we hypothesize that NQO1 has a significant effect on angiogenesis and osteogenesis by regulating mitochondrial respiration and MAPK signaling pathways in DPSCs.

In this study, we have explored the role and mechanism of NQO1 in regard to the angiogenesis and mineralization ability of DPSCs. Our study found that NQO1 inhibited angiogenesis and promoted osteogenesis of DPSCs by suppressing MAPK signaling pathways and enhancing mitochondrial respiration.

Materials and methods

DPSCs isolation and culture

The human DPSCs experiments involved in this study was approved by the Ethical Committee of Beijing Stomatological Hospital, Capital Medical University (Ethical Review NO. CMUSH-IRB-KJ-PJ-2022-22). Human premolars or third molars were obtained after obtaining informed consent. The DPSCs were obtained as described previously [25]. Use passages 3–5 of DPSCs in subsequent experiments.

HUVECs culture

HUVECs (Cat No. HUVEC-20001), and complete medium of human umbilical vein endothelial cells (HUVECs) (Cat No. HUVEC-90011), and 0.25% tryptic digestion solution (Cat. TEDTA-10001) were purchased from Cyagen Biosciences, Inc. (Guangzhou, China). Passages 5–6 of HUVECs were used in our experiments.

Plasmid construction and viral infection

Plasmid construction and viral transfection were performed as previously described [26]. Following standard methods, the plasmids were constructed and the structures were identified using restriction enzymes and sequence. The hemagglutinin (HA)-tag and human full-length NQO1 cDNA were constructed via a whole-gene synthesis method, and the HA-tag and NQO1 sequence were cloned into NheI/NotI-digested pCDH-CMV-MCS-EF1a-puro (HA-NQO1). Empty pCDH-CMV-MCS-EF1a-puro vectors was used as control (Vector). The plasmids were packaged as lentivirus. GenePharma (Suzhou, China) was responsible for synthesizing NQO1 shRNA (NQO1sh) and control shRNA (Consh). The DPSCs were then transfected by lentiviruses by using polybrene (6 μg/mL; Sigma-Aldrich, St. Louis, MO) for 12 h. The transfected DPSCs were cultured by adding 2 μg/mL puromycin after 72 h. The control group provided a reference point for the results of the experiment to better evaluate the influence of experimental conditions on the results of the experiment.

Co-culture of DPSCs and HUVECs

An Angiogenesis assay in vitro was performed as previously described [27]. Wells were coated with 50 μL Matrigel (Cat No. 356234, BD Biosciences) in a 96-well plate. 100 μL cell suspension of DPSCs and HUVECs (1×10^4 cells, respectively) was added into each well after gelatinization. After co-culture for 3 h, we obtained images with a microscope (Olympus, Japan). ImageJ software was used to quantify the tubules formed. For the sake of methodological rigor, there were three parallel wells in each group.

Scratch migration assay

The scratch migration assay was performed as described previously [26]. Changes in the width of the void area relative to that at 0 h (relative width) were evaluated in each group. In the experimental design, triplicate wells were established for both the experimental and control groups to ensure the reliability and reproducibility of the results. Within these triplicate wells, nine random fields of view were selected for microscopic examination to minimize sampling bias.

Transwell chemotaxis assay

Transwell chemotaxis assay**s** were performed as described previously [26]. After 24 and 48 h, the number of migrated cells was calculated from the micrographs. Triplicate assay conditions were implemented for both the experimental group and the control group. Within each replicate, a systematic random sampling approach was employed to select six discrete fields of view for microscopic analysis.

Angiogenesis assay in vivo

All animal experiments were performed after approval from the Animal Care and Use Committee of the Beijing Stomatological Hospital Animal Laboratory (KQYY-202212-001). Ten nude mice (female, 8-week-old, nu/nu) were obtained from the Beijing Stomatological Hospital Animal Laboratory (Beijing, China). Nude mice were anesthetized using sodium pentobarbital. 150 μL matrigel containing HUVECs and DPSCs (1×10^6 cells, respectively) was transplanted into the nude mice subcutaneously. Each nude mouse received two implants. Samples were obtained 2 weeks after transplantation. Our work has been reported in accordance with ARRIVE Guide 2.0.

Alkaline phosphatase (ALP) activity assay and Alizarin red staining (ARS)

DPSCs were induced by using osteogenic induction medium (100 μM/ml ascorbic acid, 2 mM β-glycerophosphate, 1.8 mM KH2PO4 and 10 nM dexamethasone). Using an ALP activity kit (Sigma-Aldrich) to detect ALP activity after 3 and 5 days, and Alizarin Red staining (Sigma-Aldrich) was performed after 2 weeks, as described previously [26]. Each experimental cohort was complemented with three parallel wells.

Osteogenesis assay in vivo

10 nude mice (female, 10-week-old, nu/nu) were purchased from the Beijing Stomatological Hospital Animal

(See figure on next page.)

Fig. 1 NQO1 inhibited the tubule formation ability in vitro. **A**, **B** Real-time RT-PCR **A** and western blot **B** results showed the knockdown efficiency of NQO1 in DPSCs. GAPDH was used as an internal control. **C**, **D** Micrographs of co-culture of DPSC-Consh and DPSCs-NQO1sh with HUVECs, respectively. **E–I** NQO1 knockdown increased the number of nodes (**E**), junctions (**F**)**,** segments (**G**), master segments (**H**) and meshes (**I**) formed by HUVECs. **J**, **K** Real-time RT-PCR (**J**) and western blot (**K**) results verified the over-expression efficiency of NQO1 in DPSCs. GAPDH and Vinculin were used as internal controls, respectively. **L–M** Micrograph of co-culture of DPSC-Vector and DPSCs-HA-NQO1 with HUVECs, respectively. **N–R** NQO1 over-expression decreased the number of nodes (**N**), junctions (**O**)**,** segments (**P**), master segments (**Q**) and meshes (**R**) formed by HUVECs. Student's *t*-test was performed to determine statistical significance. Error bars represent SD (n = 3). *P < 0.05; **P < 0.01. Scale bar: 500 μm (**C**, **L**), 100 μm (**D**, **M**). Full-length blots/gels are presented in Supplementary Fig. 2

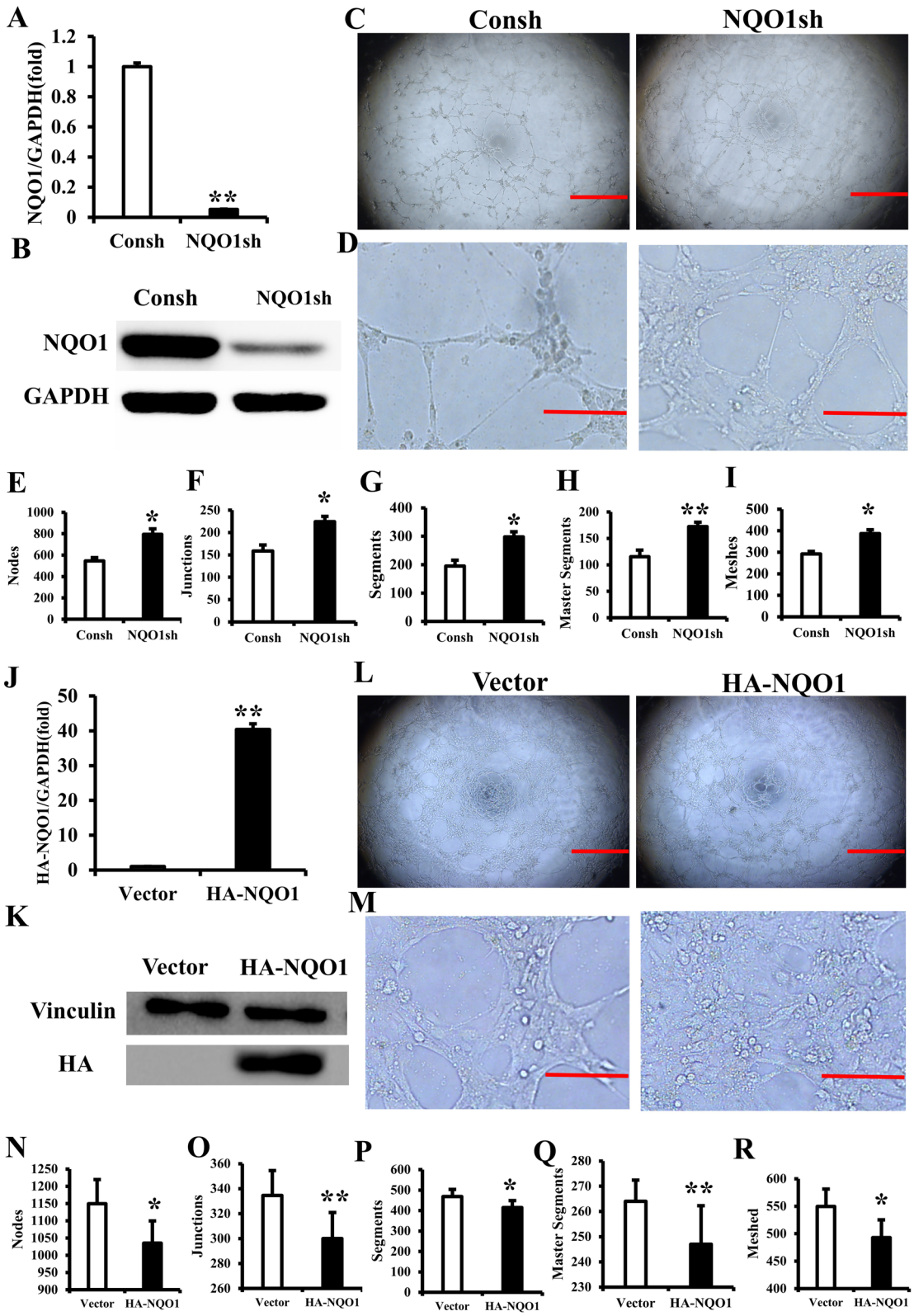

Fig. 1 (See legend on previous page.)

Laboratory (Beijing, China). None of the animals received any medical or surgical treatments. 2.0×10^6 cells were mixed with 20 mg HA/tricalcium phosphate (Engineering Research Center for Biomaterials, Chengdu, China), incubated at 37 °C for 3 h, and transplanted into the nude mice. After eight weeks, the subcutaneous grafts were removed from the back and the following experiments were performed. Our work has been reported in accordance with ARRIVE Guide 2.0.

Hematoxylin and eosin (H&E) staining

The harvested grafts were stained with H&E as described previously [27]. The number of formed vessels or mineralized tissues was analyzed. The slices were selected randomly and then generating a randomization sequence using a simple random sampling method.

Immunofluorescence staining

Immunofluorescence staining was performed as described previously [28]. Anti-CD31 primary antibody (Cat No. 11265-1-AP; Proteintech, Rosemont, IL, USA) was used for immunofluorescence staining. A fluorescence microscope (Olympus, Tokyo, Japan) was used to observe and photograph the stained samples.

Masson staining

Masson's trichrome staining was performed as described previously [29]. The newly formed osteoid were observed under a microscope (Olympus, Japan).

Immunohistochemical staining

Immunohistochemical staining was performed as described previously [26]. The primary antibodies used were anti-dentin sialophosphoprotein (DSPP; Cat No. bs-10316R; Bioss). The stained samples were observed and photographed using a microscope (Olympus, Tokyo, Japan).

Reverse transcriptase-polymerase chain reaction (RT-PCR) and real-time RT-PCR

Total RNA extraction, cDNA synthesis, and real-time RT-PCR were performed as described previously [30]. Each reaction was conducted in triplicate to ensure the reliability and consistency of the results. The primer sequences used in this study are listed in Additional file 1 (Table S1).

Western blot

Western blotting was performed as previously described [27]. The primary antibodies used were anti-NQO1 (Cat No. 11451-1-AP, Peintech, Rosemont, IL, USA), anti-DSPP (Cat No. bs-10316R, Bioss, Beijing, China), anti-Vinculin(Cat No. 26520-1-AP, Peintech, Rosemont, IL, USA), anti-HA (Cat No.51064-2-AP, Peintech, Rosemont, IL, USA), anti-JNK(Cat No. 9258; Cell Signaling Technology), anti-Phospho-JNK (Cat No. 80024-1-RR, Peintech, Rosemont, IL, USA), anti-Erk1/2 (Cat No.11257-1-AP, Peintech, Rosemont, IL, USA), anti-Phospho-Erk1/2 (Cat No.80031-1-RR, Peintech, Rosemont, IL, USA), anti-p38 (Cat No.14064-1-AP, Peintech, Rosemont, IL, USA), anti-Phospho-p38(Cat No.28796-1-AP, Peintech, Rosemont, IL, USA), SIRT1 Rabbit pAb(Cat No.A11267, Abclonal, Wuhan, China) and GAPDH (Cat No.60004-1-Ig, Peintech, Rosemont, IL, USA).

Oxygen consumption rate (OCR)

The experimental method is as described previously [31]. The DPSCs (6×10^4/well) were seeded onto XF-24 plates and the experiments were repeated three times for each group. The mitochondrial stress assay parameters were calculated by using the OCR curves. Each experimental cohort was complemented with five parallel wells.

Mitochondrial membrane potential (MMP) assay

The MMP of the DPSCs was determined using the JC-1 method (Solarbio, Beijing, China). Red fluorescence indicates a higher MMP and green fluorescence indicates a lower MMP. CCCP, an OXPHOS decoupling agent, was used as a positive control to induce MMP reduction in DPSCs. Each group was provided with three parallel wells.

Statistical analysis

All statistical analyses were performed using the SPSS 22 statistical software (SPSS Inc., Chicago, IL, USA). Student's *t*-test or one-way ANOVA was used to calculate

(See figure on next page.)

Fig. 2 NQO1 inhibited the migration and chemotaxis of DPSCs. **A**, **B** The results of scratch migration assay (**A**) and quantitative analysis (**B**) showed that NQO1 knockdown enhanced the migration of DPSCs. Error bars represent SD (n = 9). **C**, **D** The results of Transwell chemotaxis assay (**C**) and quantitative analysis (**D**) showed NQO1 knockdown improved the chemotaxis of DPSCs. Error bars represent SD (n = 6). **E**, **F** The results of scratch migration assay (**E**) and quantitative analysis (**F**) showed that NQO1 overexpression reduced the migration of DPSCs. Error bars represent SD (n = 9). **G–H** The results of Transwell chemotaxis assay (**G**) and quantitative analysis (**H**) showed that NQO1 overexpression declined the chemotaxis of DPSCs. Error bars represent SD (n = 6). Student's *t*-test was performed to determine statistical significance. *P < 0.05; **P < 0.01. Scale bar: 500 μm (**A**, **E**), 100 μm (**C**, **G**)

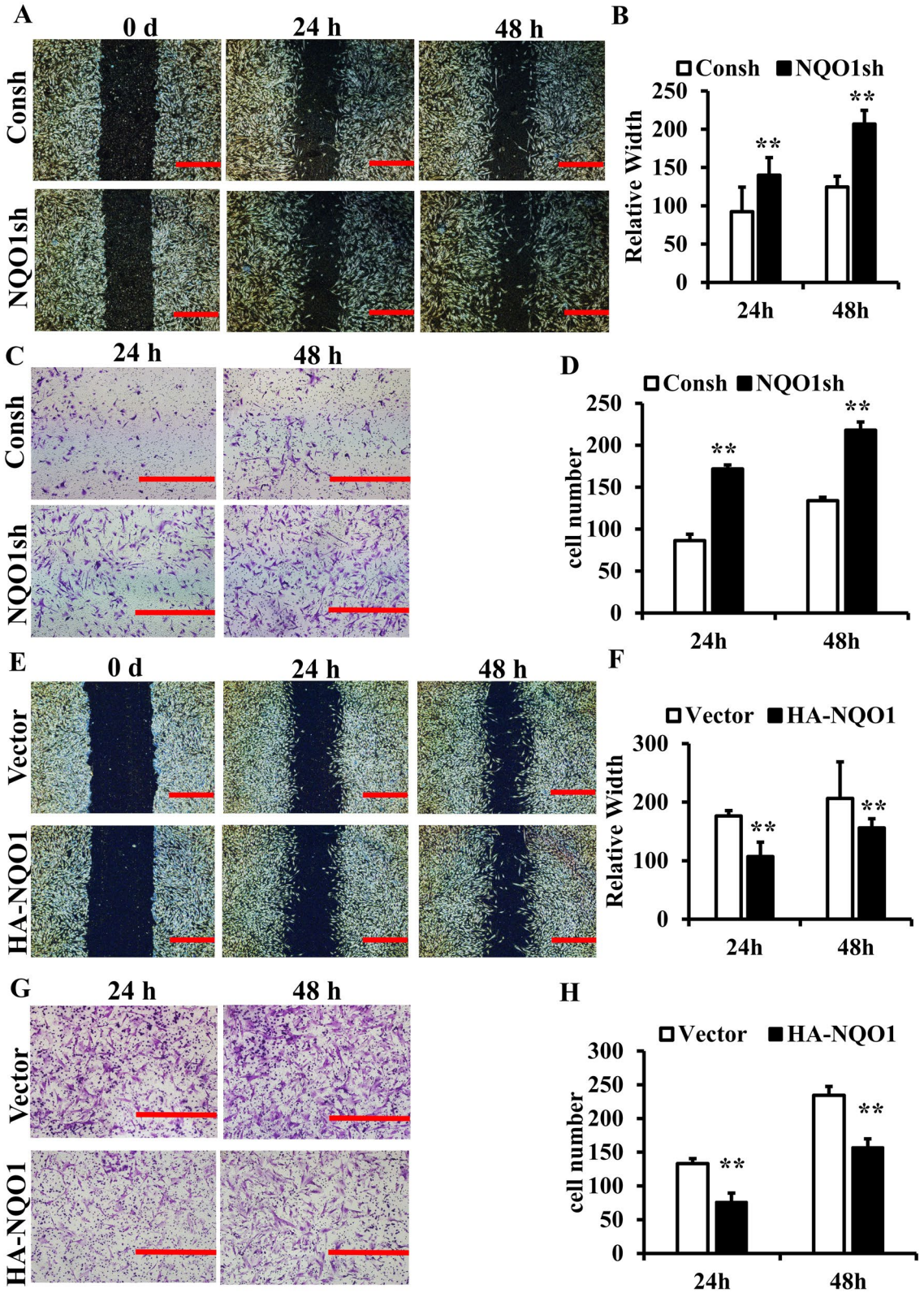

Fig. 2 (See legend on previous page.)

the data. Differences were considered statistically significant at $P < 0.05$.

Results

NQO1 inhibited the tubule formation ability in vitro

DPSCs were transfected with a lentivirus in order to establish stable NQO1 knockdown cells (DPSCs-NQO1sh) and control cells (DPSCs-Consh). Real-time RT-PCR results confirmed that NQO1 expression in DPSCs-NQO1sh was about 95% lower than that in DPSCs-Consh (Fig. 1A). The western blotting results also confirmed the successful knockdown of NQO1 (Fig. 1B). DPSCs and HUVECs (1:1 ratio) were mixed and cocultured in Matrigel for 3 h to simulate angiogenesis in vitro. The micrographs obtained showed that HUVECs co-cultured with DPSCs- NQO1sh formed more endothelial networks in the Matrigel (Fig. 1C, D). Quantitative analyses showed that NQO1 knockdown significantly increased the number of nodes (795 VS. 545), junctions (224 VS.159), segments (298 VS. 195), master segments (172 VS.115), and meshes (387 VS. 292) of the tubules formed by the HUVECs (Fig. 1E–I).

DPSCs were then transfected with the lentiviral Vector and HA-NQO1. Real-time RT-PCR results verified that the expression of NQO1 was significantly increased by about 40 times in DPSCs-HA-NQO1 compared with DPSCs-Vector (Fig. 1J). The western blotting results also confirmed the increased expression of NQO1 in DPSC- HA-NQO1 (Fig. 1K). After co-culturing for 3 h, micrographs showed that HUVECs co-cultured with DPSCs-HA-NQO1 formed fewer endothelial networks (Fig. 1L, M). More specifically, NQO1 overexpression reduced the number of nodes (1035 VS. 1149), junctions (300 VS. 334), segments (415 VS. 469), master segments (247 VS. 264), and tubule meshes (493 VS. 550), as shown by the quantitative analyses (Fig. 1N–R). These results confirmed that knockdown of NQO1 in DPSCs increased tubule formation, while overexpression of NQO1 increased tubule formation in vitro.

NQO1 inhibited the migration and chemotaxis ability of DPSCs

Scratch migration assay and quantitative analysis revealed that the migration ability of DPSCs-NQO1sh was stronger than that of DPSCs-Consh at 24 and 48 h (Fig. 2A, B). Moreover, the results of the transwell chemotaxis assay and quantitative analysis showed that DPSCs-NQO1sh had greater chemotactic ability than DPSCs-Consh at 24 and 48 h (Fig. 2C, D). For further validation, we conducted migration and chemotaxis experiments using DPSCs-HA-NQO1 and the DPSC-vector. The results showed that the overexpression of NQO1 inhibited the migration and chemotaxis of DPSCs (Fig. 2E–H). These results confirmed that NQO1 knockdown promoted the migration and chemotaxis ability of DPSCs, while overexpression of NQO1 inhibited the migration and chemotaxis ability of DPSCs.

NQO1 inhibited the angiogenesis ability of DPSCs

To determine the effect of NQO1 on angiogenesis in DPSCs, we performed animal experiments. The presented image shows a gross view of the grafts in DPSCs-Consh and DPSCs-NQO1sh (Fig. 3A). H&E staining and quantitative analysis indicated that the number of blood vessels formed in DPSCs-NQO1sh increased (Fig. 3B, C). Immunofluorescence staining showed that CD31 expression was increased in tissues formed in DPSCs-NQO1sh (Fig. 3D). We conducted the same animal experiments after NQO1 overexpression. A gross view of the grafts in DPSCs-HA-NQO1 and DPSCs-Vector is shown in Fig. 3E. The number of blood vessels formed in the DPSCs-HA-NQO1 decreased as shown by the H&E staining and quantitative analysis (Fig. 3F, G). At the same time, the immunofluorescence staining results proved that NQO1 overexpression inhibited the expression of CD31 in the new generated tissue (Fig. 3H). These results indicated that NQO1 knockdown promoted the angiogenesis of DPSCs, while NQO1 overexpression inhibited the angiogenesis of DPSCs.

NQO1 promoted osteogenesis of DPSCs in vitro and vivo

The ALP activity assay revealed that the ALP activity of DPSCs-NQO1sh was lower than that of the control group

(See figure on next page.)

Fig. 3 NQO1 inhibited the angiogenesis of DPSCs. **A** Gross view of implants taken from DPSCs-Consh group and DPSCs-NQO1sh group. **B**, **C** H&E staining (**B**) and quantitative analysis (**C**) results showed that the number of vessels in DPSCs-NQO1sh was increased when compared with the control group. **D** Immunofluorescence staining results showed that CD31 fluorescence was enhanced in DPSCs-NQO1sh. **E** Gross view of implant taken from DPSCs-Vector group and DPSCs-HA-NQO1 group. **F**, **G** H&E staining (**F**) and quantitative analysis (**G**) results showed that the number of vessels in DPSCs-HA-NQO1 was decreased when compared with the control group. **H** Immunofluorescence staining results showed that the fluorescence of CD31 was weakened after NQO1 overexpression. Student's *t*-test was performed to determine statistical significance. Error bars represent SD (n = 5). *P < 0.05. Scale bar: 20 μm (**B**, **D**, **F**, **H**). Black arow points to newly formed blood vessels (**B**, **F**)

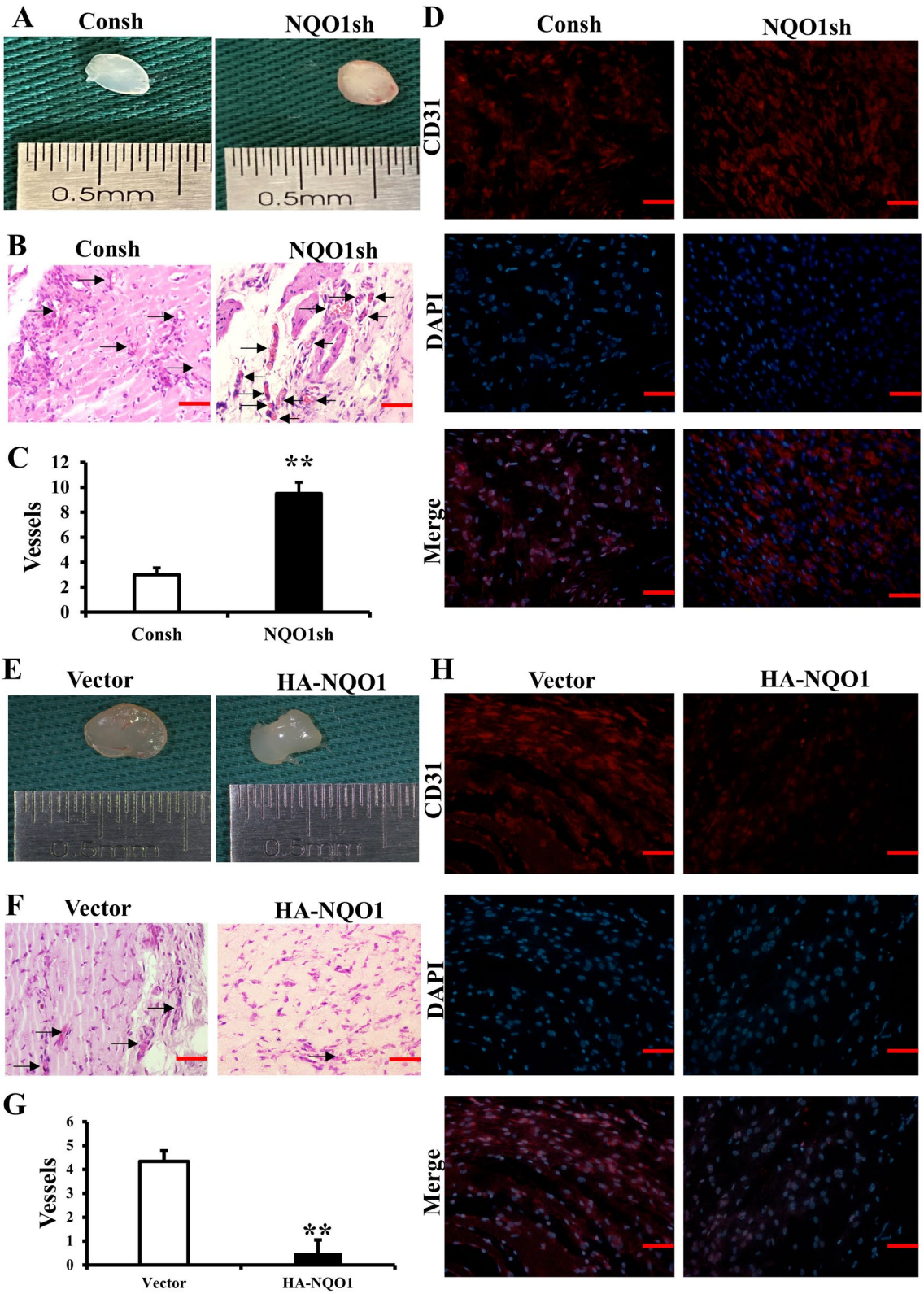

Fig. 3 (See legend on previous page.)

after 3 and 5 days of osteogenic induction (Fig. 4A, B). Alizarin Red staining indicated that NQO1 knockdown inhibited osteogenesis in vitro after 2 weeks of induction (Fig. 4C). In addition, the performed western blotting (Fig. 4D) and quantitative analysis (Fig. 4E) showed that DSPP expression was reduced in DPSCs-NQO1sh. We also performed the above experiments using DPSCs-HA-NQO1 and the DPSCs-Vector. The ALP activity of DPSCs-HA-NQO1 increased after 3 and 5 days of induction (Fig. 4F, G), and ARS staining was enhanced after 2 weeks of induction (Fig. 4H). Western blotting (Fig. 4I) and quantitative analysis (Fig. 4J) revealed that NQO1 overexpression increased DSPP expression.

We conducted animal experiments in order to reveal the effect of NQO1 on osteogenesis in vivo. Eight weeks after transplantation, both H&E (Fig. 4K, N) and Masson staining (Fig. 4L, O) results showed that the formation of the bone-like tissue in DPSCs-NQO1sh was less than that seen in the control group, whereas the formation of bone-like tissue in DPSCs-HA-NQO1was more than that seen in the control group. Moreover, the immunohistochemical staining results showed that the expression of DSPP in DPSCs-NQO1sh was lower than that in the control group, whereas the expression in DPSCs-HA-NQO1was was stronger than that in the control group (Fig. 4M, P). In conclusion, NQO1 knockdown inhibited the osteogenic ability of DPSCs, while NQO1 overexpression promoted the osteogenic ability of DPSCs in vitro and vivo.

NQO1 promoted mitochondrial respiration and increased mitochondrial membrane potential (MMP)

We used a Seahorse XFe24 analyzer to detect the effects of NQO1 on mitochondrial respiration in DPSCs. The OCR curves of the DPSCs-Consh and DPSCs-NQO1sh are presented (Fig. 5A). When compared to DPSCs-Consh, the basal oxygen consumption (105 VS. 124 pmol/min), maximal respiration (111 VS. 304 pmol/min), and Adenosine Triphosphate (ATP) production (36 VS. 85 pmol/min) of DPSCs-NQO1sh were found to be significantly decreased (Fig. 5B–D). Next, the same experiments were performed with the DPSCs-Vector and DPSCs-HA-NQO1. The OCR curves of DPSCs-Vector and DPSCs-HA-NQO1 were obtained (Fig. 5E). Basal oxygen consumption (178 VS. 147 pmol/min), maximal respiration (359 VS. 250 pmol/min), and ATP production (164 VS. 138 pmol/min) were higher in DPSCs-HA-NQO1 than those in DPSCs-Vector (Fig. 5F–H).

Additionally, the JC-1 assay was used in order to analyze the MMP in DPSCs. DPSCs-NQO1sh formed less JC-1 aggregates than DPSCs-Consh did, indicating reduced MMP level in DPSCs-NQO1sh (Fig. 5I). In contrast, DPSCs-HA-NQO1 formed more JC-1 aggregates than the control group, indicating that the MMP level of DPSCs-HA-NQO1was increased (Fig. 5J). In summary, NQO1 knockdown decreased mitochondrial respiration and MMP of DPSCs, while NQO1 overexpression increased mitochondrial respiration and MMP of DPSCs.

NQO1 inhibited tubule formation ability and promoted osteogenic differentiation of DPSCs by activating mitochondrial respiration

CoQ10, an important hydrogen transmitter in the mitochondrial electron transport chain, was added to the medium with a concentration of 30 μM, and DPSCs-NQO1sh were pretreated in the medium for 3 days. Tubule formation experiments were performed in vitro. Compared to untreated DPSCs-NQO1sh, DPSCs-NQO1sh pretreated with CoQ10 resulted in less endothelial network formation (Fig. 6A, B). Correspondingly, the number of meshes and junctions in the tubules formed by the HUVECs decreased in the CoQ10 pretreated DPSCs-NQO1sh group (Fig. 6C, D). Moreover, CoQ10 pretreatment reduced DPSCs migration (Fig. 6E, F) and their chemotactic ability (Fig. 6G, H).

CoQ10 was added to the osteogenic induction medium at a concentration of 30 μM. After 3 days of induction, CoQ10 treatment resulted in an increase in the

(See figure on next page.)

Fig. 4 NQO1 promoted calcification of DPSCs in vitro and vivo. **A**, **B** ALP activity assay showed that ALP activity decreased in DPSCs-NQO1sh after osteogenic induction for 3 days and 5 days. **C** Alizarin Red staining result showed that the mineralization of DPSCs-NQO1sh declined after 2 weeks of osteogenic induction. **D**, **E** Western blot results (**D**) and quantitative analysis (**E**) showed that DPSCs-NQO1sh weakened the expression of DSPP after 2 weeks of osteogenic induction. **F**, **G** ALP activity assay showed that ALP activity increased in DPSCs-HA-NQO1 after osteogenic induction for 3 days and 5 days. **H** Alizarin Red staining result showed that the mineralization of DPSCs-HA-NQO1 increased after 2 weeks of osteogenic induction. **I**, **J** Western blot results (**I**) and quantitative analysis (**J**) showed that DPSCs-HA-NQO1sh enhanced the expression of DSPP after 2 weeks of osteogenic induction. **K**, **L**, **N**, **O** H&E staining (**K**, **N**) and Masson staining (**L**, **O**) showed that DPSCs-NQO1sh reduced bone-like tissue formation, while DPSCs-HA-NQO1 enhanced bone-like tissue formation. B points to newly formed bone-like tissue. HA points to HA/tricalcium phosphate. **M**, **P** Immunohistochemical staining (**M**) and quantitative analysis (**P**) showed that DSPP expression was decreased in DPSCs-NQO1sh and increased in DPSCs-HA-NQO1. Black arow points to positive cells. HA points to HA/tricalcium phosphate. Error bars represent SD (n = 3). GAPDH was used as an internal control. Student's *t*-test was performed to determine statistical significance. *P < 0.05; **P < 0.01. Scale bar: 20 μm (**K**, **L**, **M**). Full-length blots/gels are presented in Supplementary Fig. 3-4

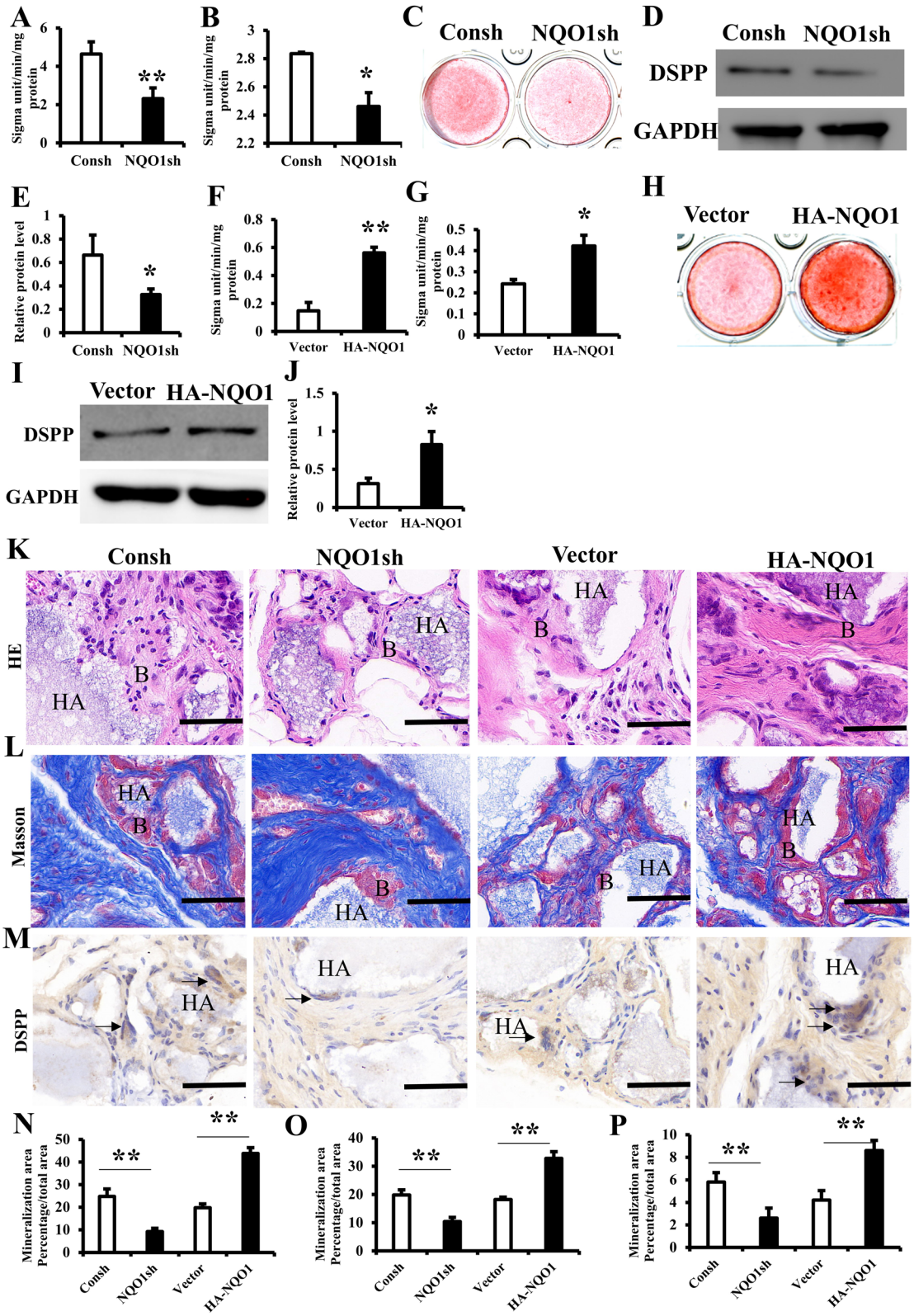

Fig. 4 (See legend on previous page.)

ALP activity of DPSCs-NQO1sh compared with that of untreated DPSCs-NQO1sh (Fig. 6I). Similarly, alizarin red staining of CoQ10 treated DPSCs-NQO1sh was enhanced after 2 weeks of induction (Fig. 6J). After rotenone (Rot), a mitochondrial respiration inhibitor, was added to osteogenic medium at a concentration of 50 nM for osteogenic induction for 3 days, the ALP activity of DPSCs-HA-NQO1 treated with Rot decreased relative to DPSCs-HA-NQO1(Fig. 6K).

NQO1 inhibited p38 MAPK, JNK and Erk1/2 signal pathways by activating mitochondrial respiration in DPSCs

To further explore the regulatory mechanism, we examined the influence of NQO1 on MAPK signaling pathways. Western blotting results showed that phospho-p38 MAPK (p-p38 MAPK), phospho-JNK (p-JNK) and phosphor-Erk1/2 (p-Erk1/2) were enhanced in DPSCs-NQO1sh compared to DPSCs-Consh, whereas there was no difference in the total protein levels of p38 MAPK, JNK, and Erk1/2 (Fig. 7A). Correspondingly, NQO1 overexpression reduced the levels of p-p38 MAPK, p-JNK, and p-Erk1/2 but had no effect on the total protein levels of p38 MAPK, JNK, and Erk1/2 (Fig. 7B). After treating DPSC-NQO1sh with 30 μM CoQ10, the enhancement effect of NQO1 knockdown on p-p38 MAPK, p-JNK and p-Erk1/2 was found to be counteracted, while the total protein levels of p38 MAPK, JNK and Erk1/2 were not affected (Fig. 7C).

NQO1 promoted the expression of SIRT1

PCR results showed that SIRT1 decreased in DPSCs-NQO1sh compared to DPSCs-Consh, but increased in DPSCs-HA-NQO1 (Supplementary Fig. 1A, B). Similarly, western blotting results showed that SIRT1 reduced in DPSCs-NQO1sh and enhanced in DPSCs-HA-NQO1 (Supplementary Fig. 1C). Therefore, in DPSCs, NQO1 knockdown reduced expression of mRNA and protein expression of SIRT1, while NQO1 overexpression increased expression of mRNA and protein expression of SIRT1.

Discussion

In cardiovascular diseases, damaged blood vessels initiate a repair process that requires angiogenesis and vascular remodeling [32]. Current treatments, including stem cell transplantation, are still immature in regard to regenerating blood vessels for the restoration of heart function. To improve angiogenesis, we investigated the function and mechanism of action of NQO1 in DPSC angiogenesis. Our results demonstrate that NQO1 inhibits tubule formation in vitro and angiogenesis in vivo. Consistent with our results, it has been reported that arsenic trioxide suppressed angiogenesis in oral squamous cell cancer cells by inducing an increase in NQO1 expression [33]. Cell migration and chemotaxis play important roles in angiogenesis [34]. Only when transplanted stem cells migrate and undergo chemotaxis around endothelial cells can they promote the formation and remodeling of new blood vessels, thereby maintaining and restoring the blood supply to the tissue. Choline increases the expression of NQO1 by activating Nrf2, thereby inhibiting vascular smooth muscle cells migration and vascular remodeling [35]. Similarly, our experiments confirmed that NQO1 inhibited the migration and chemotaxis of DPSCs, which is consistent with the inhibitory effect of NQO1 on angiogenesis.

The mineralization process of cardiovascular disease is mainly manifested by the deposition of calcium salts in the walls of blood vessels, forming calcification foci, which is consistent with the calcification process of bone formation [36]. It is beneficial to inhibit the formation of blood vessel wall calcification and reduce the occurrence of cardiovascular disease to study the influencing factors of osteogenesis and its formation mechanism. Our study demonstrated that NQO1 promotes the osteogenesis of DPSCs in vitro and in vivo, which is consistent with previous studies. Icariin has been reported to inhibit iron death in osteoblasts and promote bone formation by activating the Nrf2/HO-1/NQO1 signaling pathway [37]. It has also been reported that artesunate promotes bone formation by increasing the expression of NQO1 and inhibiting osteoclast function [38].

(See figure on next page.)

Fig. 5 NQO1 promoted mitochondrial respiration and MMP. **A** The OCR curves of DPSCs-consh and DPSCs-NQO1sh. **B–D** The basal oxygen consumption (**B**), maximal respiration (**C**) and ATP production (**D**) was reduced in DPSCs-NQO1sh. **E** The OCR curves of DPSCs-Vector and DPSCs-HA-NQO1. **F–H** The basal oxygen consumption (**F**), maximal respiration (**G**) and ATP production (**H**) was elevated in DPSCs-HA-NQO1. Error bars represent SD (n = 5). Student's *t*-test was performed to determine statistical significance. *P < 0.05; **P < 0.01. **I**, **J** JC-1 assay showed DPSCs-NQO1sh formed less JC-1 aggregates (**I**), while DPSCs-HA-NQO1 formed more JC-1 aggregates (**J**). CCCP was used as a positive control. Scale bar: 50 μm (**I**, **J**)

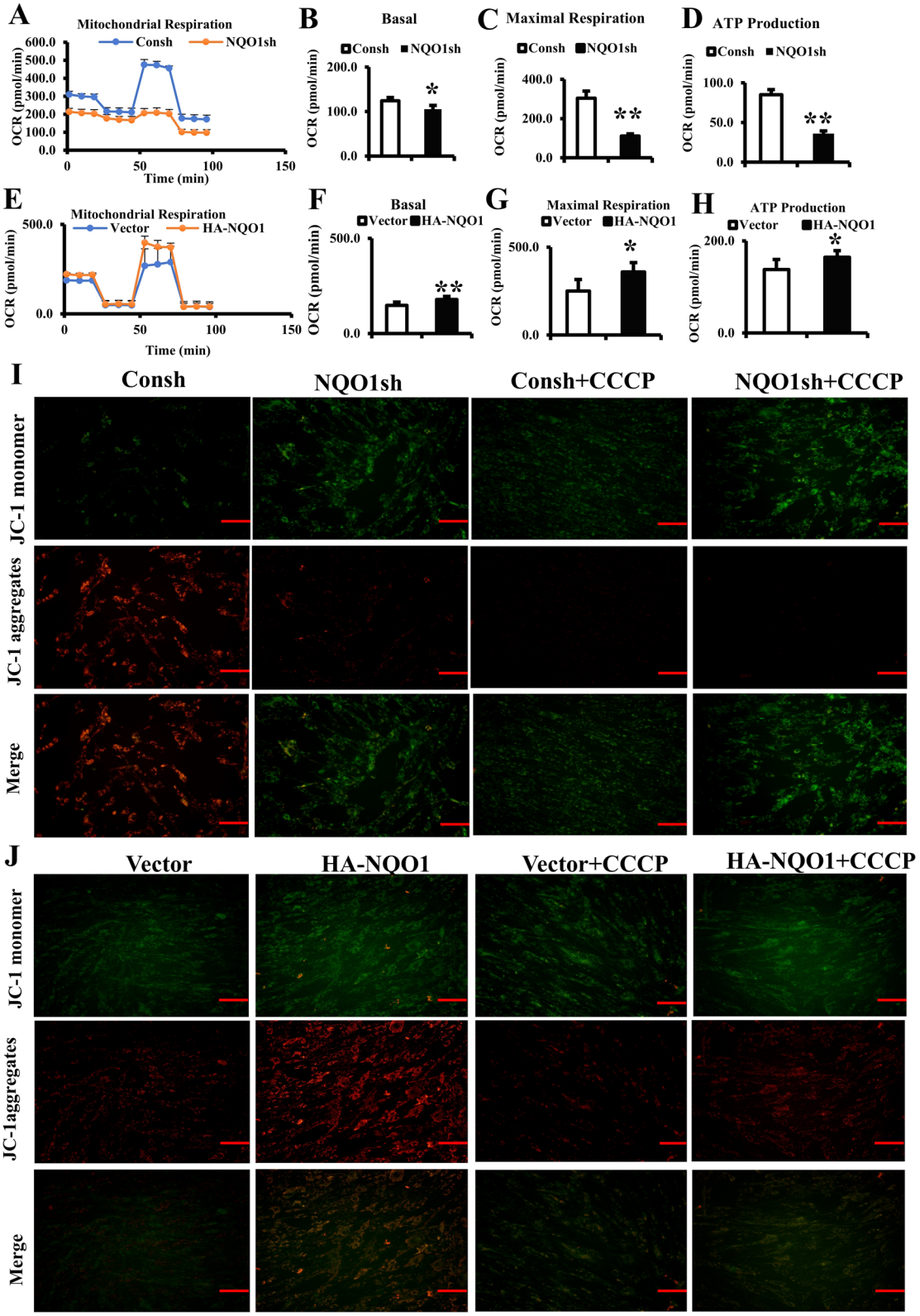

Fig. 5 (See legend on previous page.)

Next, we explored the mechanisms by which NQO1 affects angiogenesis and osteogenesis. Our results demonstrated that NQO1 promotes mitochondrial oxygen consumption and membrane potential. The higher the membrane potential, the better the mitochondrial activity, and the more vigorous the energy metabolism [39]. It has been reported that astrocyte-specific conditional deletion of mitochondrial fusion protein 2 inhibits perivascular mitochondrial aggregation, destroys the mitochondrial endoplasmic reticulum contact site, thus inhibiting vascular remodeling [40]. Platelet-derived mitochondria enhance oxidative phosphorylation through metabolic remodeling to promote angiogenic activity in stem cells [41]. FAM3A increases the production and secretion of mitochondrial adenosine triphosphate (ATP) in vascular endothelial cells, which binds to P2 receptors and upregulates cytoplasmic free Ca^{2+} levels, thereby activating VEGFA transcription and ultimately endothelial angiogenesis [42]. This study has shown that angiogenesis is promoted by enhancing mitochondrial metabolism. However, our results confirmed that NQO1 promotes mitochondrial energy metabolism and inhibits angiogenesis. This may be because NQO1 has different effects on angiogenesis in different cell types, and the specific mechanisms underlying these effects need to be further explored.

The proportion of oxidative phosphorylation in bone marrow mesenchymal stem cells increases during osteogenic differentiation [43]. In the osteoblast line MC3t3-E1 and primary cranial osteoblasts, strong mitochondrial biosynthesis and increased ATP production were observed during differentiation, and the inhibition of mitochondrial activity significantly inhibited osteoblast differentiation [44]. SIRT3 knockdown in MC3T3-E1 cells reduced the activity of the mitochondrial electron transport chain protein complexes I, II, III, IV, and V, inhibited mitochondrial oxygen consumption, reduced mitochondrial membrane potential, and inhibited osteogenic differentiation [44]. Carbon black induces mitochondrial dysfunction and leads to increased mitochondrial autophagy, ultimately resulting in the inhibition of bone formation in bone marrow mesenchymal stem cells [45]. The aforementioned literature shows that promoting mitochondrial activity will lead to the promotion of bone formation, which is consistent with our findings. Moreover, the addition of CoQ10 to DPSCs-NQO1sh reversed the changes in osteogenesis and tubule formation. These results suggested that NQO1 inhibits tubule formation and promotes osteogenesis by altering mitochondrial respiration and activity.

Mitochondria affect the MAPK signaling pathways, and the MAPK signaling pathways have an impact on angiogenesis and osteogenesis. AICAR enhances p38 MAPK phosphorylation in C2C12 cells to promote angiogenesis [46]. Soluble e-selectin [47] and migration inhibitory factor [48] significantly increased the phosphorylation of Erk1/2 and increase the angiogenesis in human dermal microvascular endothelial cells. COX-2 plays an important role in angiogenesis by enhancing the phosphorylation of p38 MAPK and JNK within HUVECs [49]. Mesenchymal stem cells regulate osteogenic differentiation by increasing p38 MAPK [50] phosphorylation. For example, G-protein coupled receptor 125 increases the expression levels of the phosphorylation of Erk and p38, and it positively regulates the formation and function of osteoclasts [51]. And after estrogen receptor α overexpression, the levels of phosphorylated Erk and JNK proteins were found to be significantly increased, which promoted the osteogenic differentiation of apical papilla stem cells [52].

We examined the expression of the MAPK signaling pathway after NQO1 knockdown and overexpression. The results showed that NQO1 inhibited the phosphorylation of Erk1/2, JNK, and p38 MAPK and promoted the osteogenesis of DPSC. The addition of CoQ10 reversed the inhibition of the MAPK signaling pathways, indicating that NQO1 inhibits the MAPK signaling pathway through the mitochondria, thereby inhibiting angiogenesis and promoting osteogenesis.

(See figure on next page.)

Fig. 6 NQO1 inhibited tubule formation and promoted osteogenic differentiation of DPSCs by activating mitochondrial respiration. **A**, **B** Micrographs of co-culture of DPSC-Consh, DPSCs-NQO1sh, and DPSCs-NQO1sh pretreated with CoQ10 with HUVECs, respectively. **C**, **D** DPSCs-NQO1sh pretreated with CoQ10 decreased the number of meshes (**C**) and junctions (**D**) formed by HUVECs when compared with untreated DPSCs-NQO1sh. Error bars represent SD (n = 3). **E**, **F** The results of scratch migration assay (**E**) and quantitative analysis (**F**) showed that DPSCs-NQO1sh pretreated with CoQ10 inhibited the migration of DPSCs when compared with untreated DPSCs-NQO1sh. Error bars represent SD (n = 9). **G**, **H** The results of Transwell chemotaxis assay (**H**) and quantitative analysis (**G**) showed DPSCs-NQO1sh pretreated with CoQ10 restrained the chemotaxis of DPSCs when compared with untreated DPSCs-NQO1sh. Error bars represent SD (n = 6). **I** ALP activity assay showed that DPSCs-NQO1sh pretreated with CoQ10 increased ALP activity after 3 days of osteogenic induction when compared with untreated DPSCs-NQO1sh. **J** Alizarin Red staining result showed that DPSCs-NQO1sh pretreated with CoQ10 increased ALP activity after 2 weeks of osteogenic induction compared with DPSCs-NQO1sh. **K** ALP activity assay showed that DPSCs-HA-NQO1 pretreated with Rot reduced ALP activity after 3 days of osteogenic induction when compared with untreated DPSCs- HA-NQO1.One-way ANOVA (**C**, **D**, **F**, **G**, **I**, **K**) were performed to determine statistical significance. *P < 0.05; **P < 0.01.Scale bar: 500 μm (**A**, **E**), 100 μm (**B**, **H**)

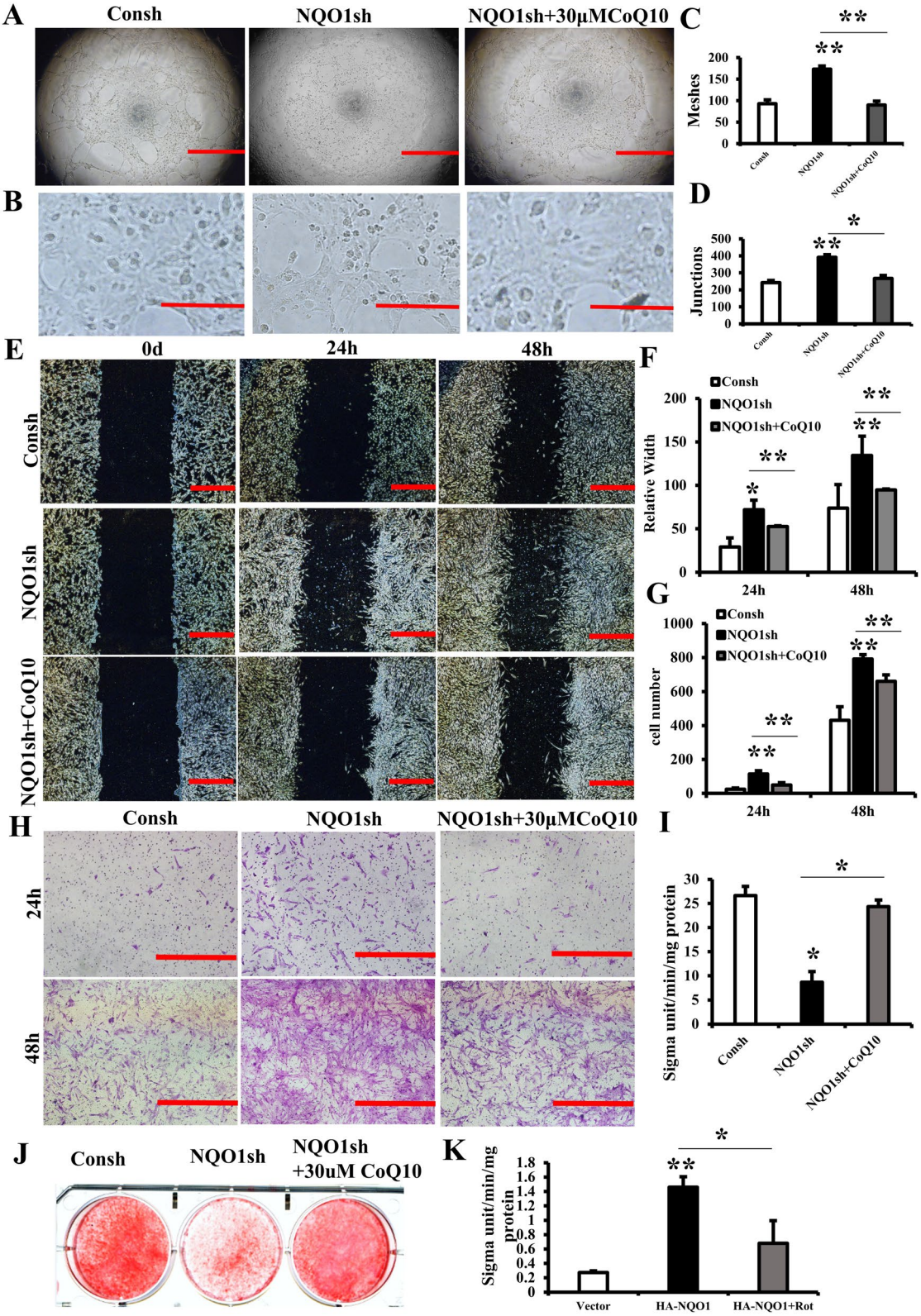

Fig. 6 (See legend on previous page.)

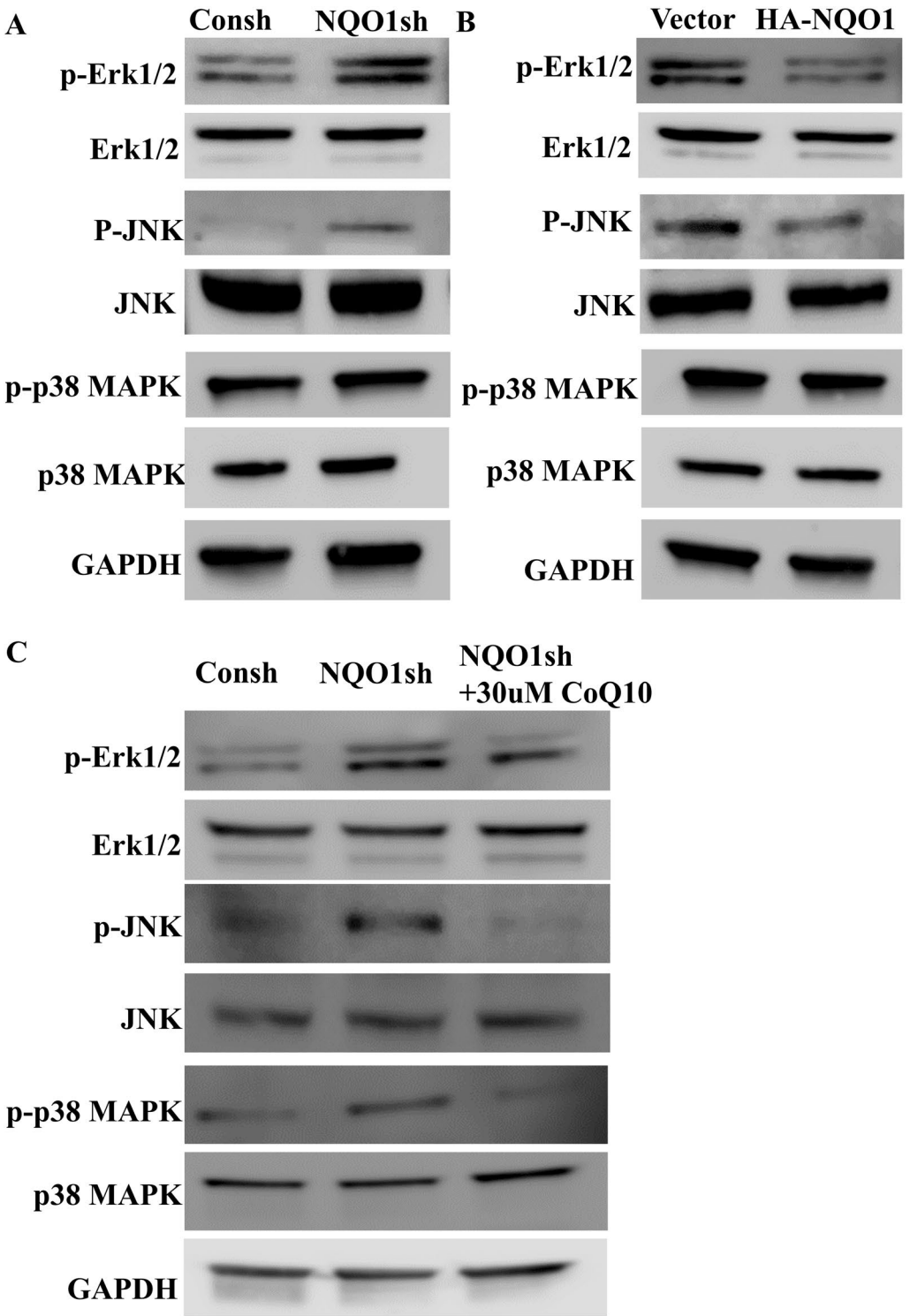

Fig. 7 NQO1 inhibited MAPK signaling pathways by activating mitochondrial respiration. **A** Western blot showed the expression of p-p38 MAPK, p-JNK and p-Erk1/2 enhanced. **B** Western blot showed the expression of p-p38 MAPK, p-JNK and p-Erk1/2 decreased. **C** Western blot showed the expression of p-p38 MAPK, p-JNK and p-Erk1/2 decreased in CoQ10 pretreated DPSCs-NQO1sh when compared with untreated DPSCs-NQO1sh. GAPDH was used as an internal control. Full-length blots/gels are presented in Supplementary Fig. 5–10

The limitations of the study are mainly reflected in the following points. Studies have only looked at the effects of NQO1 on DPSCs in the short term, but the long-term effects and potential side effects have not been fully evaluated. Although NQO1 influences angiogenesis and osteogenesis by regulating MAPK signaling pathways, the specific molecular mechanisms of how NQO1 precisely regulates these pathways need to be further elucidation. Although the research results provide a new perspective for the treatment of atherosclerosis, it is not clear how to translate these basic research results into specific strategies and methods for clinical application. According to the research results, we will explore the following aspects in the future: further mitochondrial function analysis of DPSCs with NQO1 knockdown and overexpression, including mitochondrial DNA copy number, mitochondrial biosynthesis and mitochondrial network morphology; DPSCs were treated with specific inhibitors or activators of MAPK signaling pathway to observe whether the effect of changes in NQO1 expression on angiogenesis and osteogenesis was related to the activity of MAPK signaling pathway; study the effect of NQO1 on the function of DPSCs in different physiological and pathological states to evaluate its potential and safety in clinical application.

Conclusion

In conclusion, NQO1 inhibited angiogenesis and promoted osteogenesis of DPSCs by suppressing MAPK signaling pathways and enhancing mitochondrial respiration. Our results elucidate the potential role and mechanism of NQO1 in angiogenesis and osteogenesis and also provide candidate targets for the treatment of arteriosclerosis in cardiovascular disease.

Abbreviations

ALP	Alkaline phosphatase
ARS	Alizarin red staining
ATP	Adenosine Triphosphate
CCCP	Carbonyl cyanide 3-chlorophenylhydrazone
CD31	Platelet endothelial cell adhesion molecule-1
CoQ10	Coenzyme Q10
DPSCs	Dental pulp stem cells
DSPP	Dentin Sialophosphoprotein
HUVECs	Human umbilical vein endothelial cells
MMP	Mitochondrial membrane potential
NQO1	NAD(P)H Quinone Dehydrogenase 1
p-Erk1/2	Phosphor-Erk1/2
p-JNK	Phosphor-JNK
p-p38 MAPK	Phospho-p38 MAPK
Rot	Rotenone

Supplementary Information

The online version contains supplementary material available at https://doi.org/10.1186/s13287-024-03929-4.

Supplementary Material 1.

Supplementary Material 2.

Supplementary Material 3: Supplementary Fig. 1 NQO1 promoted the expression of SIRT1. (A, B) PCR results showed that SIRT1 decreased in DPSCs-NQO1sh compared to DPSCs-Consh, but increased in DPSCs-HA-NQO1. (C) Western blotting results showed that SIRT1 reduced in DPSCs-NQO1sh and enhanced in DPSCs-HA-NQO1. Student's t-test was performed to determine statistical significance. Error bars represent SD (n = 3). **P < 0.01. GAPDH was used as an internal control. Full-length blots/gels are presented in Supplementary Fig. 11.

Supplementary Material 4.

Supplementary Material 5.

Supplementary Material 6.

Supplementary Material 7.

Supplementary Material 8.

Supplementary Material 9.

Supplementary Material 10.

Supplementary Material 11.

Supplementary Material 12.

Supplementary Material 13.

Acknowledgements

We acknowledge the reviewers for their helpful comments. The authors declare that artificial intelligence is not used in this study.

Author contributions

WW performed the experiments, participated in data collection and analysis, and drafted the manuscript. HY participated in the animal experiments and data collection. ZF was responsible for the study conception and design, manuscript revision, financial support, and final approval of the manuscript. RS participated in the data collection and analysis, study conception and design, manuscript writing, and financial support. All the authors have read and approved the final version of the manuscript.

Funding

This work was supported by grants from the National Natural Science Foundation of China (82071071 to R.T.S. and 82130028 to Z.P.F.), the National Key Research and Development Program (2022YFA1104401), the CAMS Innovation Fund for Medical Sciences (2019-I2M-5-031 to Z.P.F.), and grants from Innovation Research Team Project of Beijing Stomatological Hospital, Capital Medical University (NO. CXTD202204 to Z.P.F.).The funding agencies played no role in the design of the study; collection, analysis, and interpretation of data; or writing of the manuscript.

Availability of data and materials

The data supporting the conclusions of this article are all online.

Declarations

Ethics approval and consent to participate

The experiments involving human DPSCs in this study have been approved by the Ethical Committee of Beijing Stomatological Hospital, Capital Medical University (Title: Effect and mechanism of the STL-NQO1 signaling pathway on the function of dental pulp stem cells and dentin regeneration under hypoxic conditions; Ethical Review No. CMUSH-IRB-KJ-PJ-2022-22; Date of approval: 2022-7-15). This study was adhered to the tenants of the Declaration of Helsinki. Human third molars or premolars were obtained with informed patient consent. DPSCs were cultured and used from passages 3–5 in our experiments. The patients provided written informed consent for the use of the samples. The animal experiment was approved by the Animal Ethics Committee of the Beijing Stomatological Hospital of the Capital Medical University (Title: Effect and mechanism of NQO1 on osteogenic and angiogenic differentiation of dental pulp stem cells; Approval number: KQYY-202309-007; Date of approval: 2023-10-18). In animal experiments, we euthanized experimental animals with cervical dislocation.

Consent for publication
Not applicable.

Competing interests
The authors declare that they have no competing interests.

Received: 4 June 2024 Accepted: 6 September 2024
Published online: 16 September 2024

References

1. Akoumianakis I, Polkinghorne M, Antoniades C. Non-canonical WNT signalling in cardiovascular disease: mechanisms and therapeutic implications. Nat Rev Cardiol. 2022;19(12):783–97. https://doi.org/10.1038/s41569-022-00718-5.
2. Tölle M, Reshetnik A, Schuchardt M, Höhne M, van der Giet M. Arteriosclerosis and vascular calcification: causes, clinical assessment and therapy. Eur J Clin Invest. 2015;45(9):976–85. https://doi.org/10.1111/eci.12493.
3. Andrus EC, Allen EV, Merritt HH, Duff GL, Moore RA, Kendall FE, et al. The pathogenesis of arteriosclerosis. Int J Epidemiol. 2015;44(6):1791–3. https://doi.org/10.1093/ije/dyv347.
4. Zhang C, Huang L, Wang X, Zhou X, Zhang X, Li L, et al. Topical and intravenous administration of human umbilical cord mesenchymal stem cells in patients with diabetic foot ulcer and peripheral arterial disease: a phase I pilot study with a 3-year follow-up. Stem Cell Res Ther. 2022;13(1):451. https://doi.org/10.1186/s13287-022-03143-0.
5. Zhang H, Wan X, Tian J, An Z, Liu L, Zhao X, et al. The therapeutic efficacy and clinical translation of mesenchymal stem cell-derived exosomes in cardiovascular diseases. Biomed Pharmacother. 2023;167: 115551. https://doi.org/10.1016/j.biopha.2023.115551.
6. Gandia C, Armiñan A, García-Verdugo JM, Lledó E, Ruiz A, Miñana MD, et al. Human dental pulp stem cells improve left ventricular function, induce angiogenesis, and reduce infarct size in rats with acute myocardial infarction. Stem Cells. 2008;26(3):638–45. https://doi.org/10.1634/stemcells.2007-0484.
7. Jashire Nezhad N, Safari A, Namavar MR, Nami M, Karimi-Haghighi S, Pandamooz S, et al. Short-term beneficial effects of human dental pulp stem cells and their secretome in a rat model of mild ischemic stroke. J Stroke Cerebrovasc Dis. 2023;32(8): 107202. https://doi.org/10.1016/j.jstrokecerebrovasdis.2023.107202.
8. Yu X, Liu J, Zhu H, Xia Y, Gao L, Dong Y, et al. Synergistic association of DNA repair relevant gene polymorphisms with the risk of coronary artery disease in northeastern Han Chinese. Thromb Res. 2014;133(2):229–34. https://doi.org/10.1016/j.thromres.2013.11.017.
9. Wittkopp S, Staimer N, Tjoa T, Stinchcombe T, Daher N, Schauer JJ, et al. Nrf2-related gene expression and exposure to traffic-related air pollution in elderly subjects with cardiovascular disease: An exploratory panel study. J Expo Sci Environ Epidemiol. 2016;26(2):141–9. https://doi.org/10.1038/jes.2014.84.
10. Ross D, Siegel D. The diverse functionality of NQO1 and its roles in redox control. Redox Biol. 2021;41: 101950. https://doi.org/10.1016/j.redox.2021.101950.
11. Zhang X, Leng S, Liu X, Hu X, Liu Y, Li X, et al. Ion channel Piezo1 activation aggravates the endothelial dysfunction under a high glucose environment. Cardiovasc Diabetol. 2024;23(1):150. https://doi.org/10.1186/s12933-024-02238-7.
12. Pantan R, Tocharus J, Suksamrarn A, Tocharus C. Synergistic effect of atorvastatin and Cyanidin-3-glucoside on angiotensin II-induced inflammation in vascular smooth muscle cells. Exp Cell Res. 2016;342(2):104–12. https://doi.org/10.1016/j.yexcr.2016.02.017.
13. Harada N, Ito K, Hosoya T, Mimura J, Maruyama A, Noguchi N, et al. Nrf2 in bone marrow-derived cells positively contributes to the advanced stage of atherosclerotic plaque formation. Free Radic Biol Med. 2012;53(12):2256–62. https://doi.org/10.1016/j.freeradbiomed.2012.10.001.
14. Zhang M, Huang SS, He WY, Cao WJ, Sun MY, Zhu NW. Nasal administration of bFGF-loaded nanoliposomes attenuates neuronal injury and cognitive deficits in mice with vascular dementia induced by repeated cerebral ischemia-reperfusion. Int J Nanomed. 2024;19:1431–50. https://doi.org/10.2147/IJN.S452045.
15. Wang K, Zhou C, Li L, Dai C, Wang Z, Zhang W, et al. Aucubin promotes bone-fracture healing via the dual effects of anti-oxidative damage and enhancing osteoblastogenesis of hBM-MSCs. Stem Cell Res Ther. 2022;13(1):424. https://doi.org/10.1186/s13287-022-03125-2.
16. Gao J, Xiang S, Wei X, Yadav RI, Han M, Zheng W, et al. Icariin promotes the osteogenesis of bone marrow mesenchymal stem cells through regulating sclerostin and activating the Wnt/β-catenin signaling pathway. Biomed Res Int. 2021;2021:6666836. https://doi.org/10.1155/2021/6666836.
17. Ross D, Zhou H, Siegel D. Benzene toxicity: the role of the susceptibility factor NQO1 in bone marrow endothelial cell signaling and function. Chem Biol Interact. 2011;192(1–2):145–9. https://doi.org/10.1016/j.cbi.2010.10.008.
18. Wu PY, Lai SY, Su YT, Yang KC, Chau YP, Don MJ, et al. β-Lapachone, an NQO1 activator, alleviates diabetic cardiomyopathy by regulating antioxidant ability and mitochondrial function. Phytomedicine. 2022;104:154255. https://doi.org/10.1016/j.phymed.2022.154255.
19. Suh J, Kim NK, Shim W, Lee SH, Kim HJ, Moon E, et al. Mitochondrial fragmentation and donut formation enhance mitochondrial secretion to promote osteogenesis. Cell Metab. 2023;35(2):345-360.e7. https://doi.org/10.1016/j.cmet.2023.01.003.
20. Cai W, Zhang J, Yu Y, Ni Y, Wei Y, Cheng Y, et al. Mitochondrial transfer regulates cell fate through metabolic remodeling in osteoporosis. Adv Sci (Weinh). 2023;10(4): e2204871. https://doi.org/10.1002/advs.202204871.
21. Wang C, Dai X, Wu S, Xu W, Song P, Huang K. FUNDC1-dependent mitochondria-associated endoplasmic reticulum membranes are involved in angiogenesis and neoangiogenesis. Nat Commun. 2021;12(1):2616. https://doi.org/10.1038/s41467-021-22771-3.
22. Zhang M, Zhang S. Mitogen-activated protein kinase cascades in plant signaling. J Integr Plant Biol. 2022;64(2):301–41. https://doi.org/10.1111/jipb.13215.
23. Wang T, Zhao H, Jing S, Fan Y, Sheng G, Ding Q, et al. Magnetofection of miR-21 promoted by electromagnetic field and iron oxide nanoparticles via the p38 MAPK pathway contributes to osteogenesis and angiogenesis for intervertebral fusion. J Nanobiotechnology. 2023;21(1):27. https://doi.org/10.1186/s12951-023-01789-3.
24. Lim JH, Lee JI, Suh YH, Kim W, Song JH, Jung MH. Mitochondrial dysfunction induces aberrant insulin signalling and glucose utilisation in murine C2C12 myotube cells. Diabetologia. 2006;49(8):1924–36. https://doi.org/10.1007/s00125-006-0278-4.
25. Zheng H, Wang N, Li L, Ge L, Jia H, Fan Z. miR-140-3p enhanced the osteo/odontogenic differentiation of DPSCs via inhibiting KMT5B under hypoxia condition. Int J Oral Sci. 2021;13(1):41. https://doi.org/10.1038/s41368-021-00148-y.
26. Yang H, Liang Y, Cao Y, Cao Y, Fan Z. Homeobox C8 inhibited the osteo-/dentinogenic differentiation and migration ability of stem cells of the apical papilla via activating KDM1A. J Cell Physiol. 2020;235(11):8432–45. https://doi.org/10.1002/jcp.29687.
27. Wang W, Yang H, Fan Z, Shi R. STL inhibited angiogenesis of DPSCs through depressing mitochondrial respiration by enhancing RNF217. Adv Biol (Weinh). 2024. https://doi.org/10.1002/adbi.202400042.
28. Diao S, Yang H, Cao Y, Yang D, Fan Z. IGF2 enhanced the osteo-/dentinogenic and neurogenic differentiation potentials of stem cells from apical papilla. J Oral Rehabil. 2020;47(Suppl 1):55–65. https://doi.org/10.1111/joor.12859.
29. García-López J, Garciadiego-Cázares D, Melgarejo-Ramírez Y, Sánchez-Sánchez R, Solís-Arrieta L, García-Carvajal Z, et al. Chondrocyte differentiation for auricular cartilage reconstruction using a chitosan based hydrogel. Histol Histopathol. 2015;30(12):1477–85. https://doi.org/10.14670/HH-11-642.
30. Qin Q, Yang H, Zhang C, Han X, Guo J, Fan Z, et al. lncRNA HHIP-AS1 promotes the osteogenic differentiation potential and inhibits the migration ability of periodontal ligament stem cells. Stem Cells Int. 2021;2021:5595580. https://doi.org/10.1155/2021/5595580.
31. Yan W, Li L, Ge L, Zhang F, Fan Z, Hu L. The cannabinoid receptor I (CB1) enhanced the osteogenic differentiation of BMSCs by rescue impaired mitochondrial metabolism function under inflammatory condition. Stem Cell Res Ther. 2022;13(1):22. https://doi.org/10.1186/s13287-022-02702-9.

32. Lu Y, Leng Y, Li Y, Wang J, Wang W, Wang R, et al. Endothelial RIPK1 protects artery bypass graft against arteriosclerosis by regulating SMC growth. Sci Adv. 2023;9(35):eadh8939. https://doi.org/10.1126/sciadv.adh8939.
33. Zhang X, Su Y, Zhang M, Sun Z. Opposite effects of arsenic trioxide on the Nrf2 pathway in oral squamous cell carcinoma in vitro and in vivo. Cancer Lett. 2012;318(1):93–8. https://doi.org/10.1016/j.canlet.2011.12.005.
34. Liu J, Long X, Li H, Yan Q, Wang L, Qin Z, et al. C1q/TNF-related protein 4 mediates proliferation and migration of vascular smooth muscle cells during vascular remodelling. Clin Transl Med. 2023;13(5): e1261. https://doi.org/10.1002/ctm2.1261.
35. He X, Deng J, Yu XJ, Yang S, Yang Y, Zang WJ. Activation of M3AChR (type 3 muscarinic acetylcholine receptor) and nrf2 (nuclear factor erythroid 2-related factor 2) signaling by choline alleviates vascular smooth muscle cell phenotypic switching and vascular remodeling. Arterioscler Thromb Vasc Biol. 2020;40(11):2649–64. https://doi.org/10.1161/ATVBAHA.120.315146.
36. Lee JS, Morrisett JD, Tung CH. Detection of hydroxyapatite in calcified cardiovascular tissues. Atherosclerosis. 2012;224(2):340–7. https://doi.org/10.1016/j.atherosclerosis.2012.07.023.
37. Xiang S, Zhao L, Tang C, Ling L, Xie C, Shi Y, et al. Icariin inhibits osteoblast ferroptosis via Nrf2/HO-1 signaling and enhances healing of osteoporotic fractures. Eur J Pharmacol. 2024;965: 176244. https://doi.org/10.1016/j.ejphar.2023.176244.
38. Su X, Guo W, Yuan B, Wang D, Liu L, Wu X, et al. Artesunate attenuates bone erosion in rheumatoid arthritis by suppressing reactive oxygen species via activating p62/Nrf2 signaling. Biomed Pharmacother. 2021;137: 111382. https://doi.org/10.1016/j.biopha.2021.111382.
39. Sheng N, Zhang Z, Zheng H, Ma C, Li M, Wang Z, et al. Scutellarin rescued mitochondrial damage through ameliorating mitochondrial glucose oxidation via the Pdk-Pdc axis. Adv Sci (Weinh). 2023;10(32): e2303584. https://doi.org/10.1002/advs.202303584.
40. Göbel J, Engelhardt E, Pelzer P, Sakthivelu V, Jahn HM, Jevtic M, et al. Mitochondria-endoplasmic reticulum contacts in reactive astrocytes promote vascular remodeling. Cell Metab. 2020;31(4):791-808.e8. https://doi.org/10.1016/j.cmet.2020.03.005.
41. Levoux J, Prola A, Lafuste P, Gervais M, Chevallier N, Koumaiha Z, et al. Platelets facilitate the wound-healing capability of mesenchymal stem cells by mitochondrial transfer and metabolic reprogramming. Cell Metab. 2021;33(2):283-299.e9. https://doi.org/10.1016/j.cmet.2020.12.006.
42. Xu W, Liang M, Zhang Y, Huang K, Wang C. Endothelial FAM3A positively regulates post-ischaemic angiogenesis. EBioMedicine. 2019;43:32–42. https://doi.org/10.1016/j.ebiom.2019.03.038.
43. Li Q, Gao Z, Chen Y, Guan MX. The role of mitochondria in osteogenic, adipogenic and chondrogenic differentiation of mesenchymal stem cells. Protein Cell. 2017;8(6):439–45. https://doi.org/10.1007/s13238-017-0385-7.
44. Gao J, Feng Z, Wang X, Zeng M, Liu J, Han S, et al. SIRT3/SOD2 maintains osteoblast differentiation and bone formation by regulating mitochondrial stress. Cell Death Differ. 2018;25(2):229–40. https://doi.org/10.1038/cdd.2017.144.
45. Shen Y, Wu L, Qin D, Xia Y, Zhou Z, Zhang X, et al. Carbon black suppresses the osteogenesis of mesenchymal stem cells: the role of mitochondria. Part Fibre Toxicol. 2018;15(1):16. https://doi.org/10.1186/s12989-018-0253-5.
46. Ouchi N, Shibata R, Walsh K. AMP-activated protein kinase signaling stimulates VEGF expression and angiogenesis in skeletal muscle. Circ Res. 2005;96(8):838–46. https://doi.org/10.1161/01.RES.0000163633.10240.3b.
47. Kumar P, Amin MA, Harlow LA, Polverini PJ, Koch AE. Src and phosphatidylinositol 3-kinase mediate soluble E-selectin-induced angiogenesis. Blood. 2003;101(10):3960–8. https://doi.org/10.1182/blood-2002-04-1237.
48. Amin MA, Volpert OV, Woods JM, Kumar P, Harlow LA, Koch AE. Migration inhibitory factor mediates angiogenesis via mitogen-activated protein kinase and phosphatidylinositol kinase. Circ Res. 2003;93(4):321–9. https://doi.org/10.1161/01.RES.0000087641.56024.DA.
49. Wu G, Luo J, Rana JS, Laham R, Sellke FW, Li J. Involvement of COX-2 in VEGF-induced angiogenesis via P38 and JNK pathways in vascular endothelial cells. Cardiovasc Res. 2006;69(2):512–9. https://doi.org/10.1016/j.cardiores.2005.09.019.
50. Sonowal H, Kumar A, Bhattacharyya J, Gogoi PK, Jaganathan BG. Inhibition of actin polymerization decreases osteogeneic differentiation of mesenchymal stem cells through p38 MAPK pathway. J Biomed Sci. 2013;20(1):71. https://doi.org/10.1186/1423-0127-20-71.
51. Tang CY, Wang H, Zhang Y, Wang Z, Zhu G, McVicar A, et al. GPR125 positively regulates osteoclastogenesis potentially through AKT-NF-κB and MAPK signaling pathways. Int J Biol Sci. 2022;18(6):2392–405. https://doi.org/10.7150/ijbs.70620.
52. Wang Y, Lu Y, Li Z, Zhou Y, Gu Y, Pang X, et al. Oestrogen receptor α regulates the odonto/osteogenic differentiation of stem cells from apical papilla via ERK and JNK MAPK pathways. Cell Prolif. 2018;51(6): e12485. https://doi.org/10.1111/cpr.12485.

Publisher's Note